
Learning Embeddings for Sequential Tasks Using Population of Agents

Mridul Mahajan
MPI-SWS, Germany
mrmahaja@mpi-sws.org

Georgios Tzannetos
MPI-SWS, Germany
gtzannet@mpi-sws.org

Goran Radanovic
MPI-SWS, Germany
gradanovic@mpi-sws.org

Adish Singla
MPI-SWS, Germany
adishs@mpi-sws.org

Abstract

We present an information-theoretic framework to learn fixed-dimensional embeddings for tasks in reinforcement learning. We leverage the idea that two tasks are similar to each other if observing an agent’s performance on one task reduces our uncertainty about its performance on the other. This intuition is captured by our information-theoretic criterion which uses a diverse population of agents to measure similarity between tasks in sequential decision-making settings. In addition to qualitative assessment, we empirically demonstrate the effectiveness of our techniques based on task embeddings by quantitative comparisons against strong baselines on two application scenarios: predicting an agent’s performance on a test task by observing its performance on a small quiz of tasks, and selecting tasks with desired characteristics from a given set of options.

1 Introduction

Embeddings are widely used to represent data points as vectors in a space that captures meaningful relations between them [1–6]. They could also be utilized as representations for tasks, which has been studied in areas such as multi-task learning [7], meta-learning [8], and domain-adaptation [9].

In reinforcement learning, task embeddings could be used to understand the shared structure in sequential decision-making problems if similar tasks are embedded close to each other. Essentially, there is an underlying notion of skills required to solve sequential tasks, and several of these tasks require some skills in common. For example, consider the tasks shown in Figure 1. Each of these requires the agent to pick-up certain keys to unlock the door. The door in task s_1 requires the green key and the blue key, while the door in task s_2 requires the yellow key and the blue key. Thus, these tasks require the common skills of navigation, and picking the blue key.

Despite the potential benefits, prior work on learning task embeddings in reinforcement learning [10–22] does not explicitly optimize for task similarity. This could primarily be attributed to the lack of a general framework to measure (and reason about) similarities between sequential tasks.

To this end, we introduce an information-theoretic framework to learn fixed-dimensional embeddings for sequential tasks in reinforcement learning; the inner product in the embedding space captures similarity between tasks, and the norm of the embedding induces an ordering on the tasks based on their difficulties (see Figure 1). A critical component of the framework is a population of agents that exhibit a diverse set of behaviors. Our framework leverages the idea that two sequential tasks are similar to each other if observing the performance of an agent from this population on one

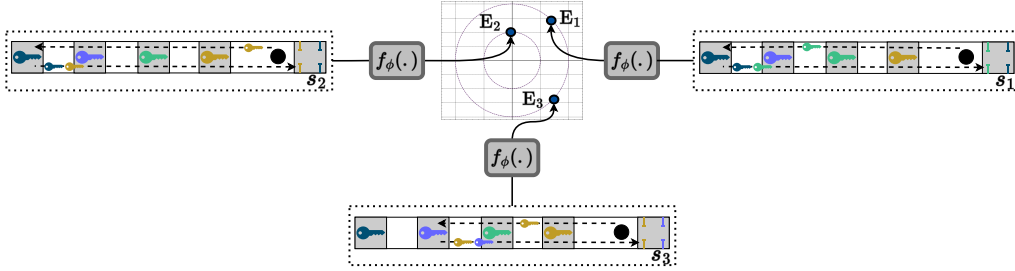


Figure 1: Schematics of our approach. We learn a task embedding function $f_\phi(\cdot)$ that maps a task s to its fixed-dimensional representation E . In this illustration, we show the properties of the learnt embeddings using the MULTIKEYNAV environment in which tasks require the agent (shown as a black circle) to pick-up certain keys (from the grey segments) to unlock the door (the right-most segment) that has certain requirements (shown in color in the form of gates). A possible solution trajectory is depicted using dotted lines. Keys on this trajectory correspond to the ones that the agent possesses at that point in time. For instance, in task s_2 , the agent starts off with the yellow key in possession already. $\langle E_1, E_2 \rangle$ is greater than $\langle E_1, E_3 \rangle$, since tasks s_1 and s_2 have a common requirement of picking the blue key, and thus, are similar. Additionally, $\|E_2\|_2$ is less than both $\|E_1\|_2$ and $\|E_3\|_2$, since task s_2 requires picking a single key, while tasks s_1 and s_3 require picking two keys, which makes them harder than s_2 .

task significantly decreases our uncertainty about its performance on the other. Concretely, we introduce an information-theoretic criterion to measure task similarity (Section 4.1), and an algorithm to empirically estimate it (Section 4.2). Through this, we construct a set of ordinal constraints on the embeddings (with each such constraint asserting the relative similarity between a triplet of tasks), and propose a training scheme for an embedding network to learn them (Section 4.3).

In addition to qualitative assessment (Section 5), we ground our framework in two downstream scenarios that are inspired by real-world applications such as performance prediction, task selection, and black-box curriculum design (Section 6). Firstly, we show the utility of our framework in predicting an agent’s performance on a new task given its performance on a small quiz of tasks. Secondly, we demonstrate the application of our framework in selecting tasks with desired characteristics from a given set of options. Through comparisons with strong baselines on a diverse set of environments, we show the efficacy of our techniques based on task embeddings.

To summarize, our work makes the following key contributions:

- I. We introduce an information-theoretic framework to learn task embeddings in reinforcement learning. As part of the framework, we propose a task similarity criterion which uses a diverse population of agents to measure similarity between sequential tasks (Section 4.1 and 4.2).
- II. We propose a scheme to learn task embeddings by leveraging the ordinal constraints imposed by our similarity criterion (Section 4.3).
- III. To assess our framework, we qualitatively investigate the learnt embedding spaces, and introduce two quantitative benchmarks: (a) agent’s performance prediction, and (b) task selection with desired characteristics (Section 5 and 6).¹

2 Related Work

Task embeddings in supervised learning. The TASK2VEC framework [8] can be used to obtain embeddings for visual classification tasks, where the embedding is the Fisher information matrix (FIM) associated with the probe network’s parameters (pre-trained on the ImageNet dataset). [23] shows the versatility of this framework by using it to obtain embeddings for NLP tasks, with the language representation model BERT [24] as the probe network. In contrast to architecture-dependent methods, [25] proposes a framework to learn task embeddings for classification problems using the optimal transport theory. Given the fundamental differences between supervised learning and reinforcement learning, these methods are not applicable in our setting.

¹Github repo: <https://github.com/machine-teaching-group/task-embeddings-rl>.

Embeddings in reinforcement learning. Embeddings are generally used in reinforcement learning to aid generalization [26–33]. For instance, [26] introduces policy similarity metric (PSM) for measuring behavioral similarity between states and uses it to learn state representations. Some works, such as [33], also learn action embeddings for sample-efficient policy learning.

Task embeddings in reinforcement learning. Several works in the meta-learning and multi-task learning literature have explored the use of task embeddings to model relationships between sequential tasks, where embeddings are either learnt explicitly through objectives such as reconstruction [12, 13, 15] and trajectory-based contrastive learning [17, 18], or implicitly to aid generalization to new tasks [19–22]. However, the reconstruction objective is not ideal for learning task embeddings as superficial differences in states could lead to similar tasks being embedded far apart. In addition, techniques that use trajectory-based contrastive learning to learn task embeddings merely aim to obtain distinct clusters for each task, without considering task similarity. Further, techniques that learn task embeddings implicitly may not be explicitly optimizing for task similarity. In contrast, our work introduces a theoretically motivated measure of task similarity and constructs an explicit objective to learn task embeddings using the similarity criterion.

Population-based techniques. Our framework requires access to a diverse population of agents. This is inline with [30, 34–37], which use a population of agents in the reinforcement learning setting. For example, [34] uses a randomly generated agent population to empirically estimate *policy information capacity*, an information-theoretic measure of task difficulty in reinforcement learning.

3 Problem Setup

MDP and Tasks. We use the Markov Decision Process (MDP) framework to define an environment. An MDP \mathcal{M} is defined as a 6-tuple $(\mathcal{S}, \mathcal{A}, \mathcal{R}, \mathcal{T}, \mathcal{S}_{\text{init}}, \gamma)$, where \mathcal{S} is the state space, \mathcal{A} is the action space, $\mathcal{R} : \mathcal{S} \times \mathcal{A} \rightarrow \mathbb{R}$ is the reward function, $\mathcal{T} : \mathcal{S} \times \mathcal{S} \times \mathcal{A} \rightarrow [0, 1]$ is the transition dynamics, and $\mathcal{S}_{\text{init}} \subseteq \mathcal{S}$ is the set of initial states. Each state $s \in \mathcal{S}_{\text{init}}$ corresponds to a goal-based task (for example, the goal could be to reach a specific destination in a navigation task) where the reward is 0 on all transitions but those on which a task gets completed. On task completion, the reward is 1. As an alternative to discounting, at each time step, there is a failure probability of $1 - \gamma$, which incentivises the agent to solve the task quickly. This ensures that the cumulative reward is binary.

Population of agents and task solvability. $p(\theta)$ represents a distribution over the population of agents. Concretely, it is a distribution over the agents’ policy parameters. We use Θ to represent the random variable that takes on the value θ . $\mathcal{O}_{s,\Theta} \in \{0, 1\}$ is a Bernoulli random variable that takes on the value 1 if, on a rollout, an agent sampled from $p(\theta)$ could successfully solve the task $s \in \mathcal{S}_{\text{init}}$ (i.e., the cumulative reward is 1), and 0 otherwise. We call $\mathcal{O}_{s,\Theta}$ the optimality variable for task s . $\text{POS}(s) := \mathbb{E}[\mathcal{O}_{s,\Theta}]$ denotes the probability of success on s , and is the complement of task difficulty.

Task embedding space. Formally, we wish to learn a task embedding function (parameterized by ϕ) $f_\phi : \mathcal{S}_{\text{init}} \rightarrow \mathbb{R}^n$, for an MDP \mathcal{M} and a prior over the population of agents $p(\theta)$, that maps tasks to n -dimensional representations. The range of $f_\phi(\cdot)$ is the task embedding space.

Objective. Our objective is to learn embeddings for sequential tasks with the following properties: (a) the inner product in the embedding space captures similarity between tasks, where the realizations of optimality variables are similar for tasks that are embedded close to each other, and (b) the norm of the embedding induces an ordering on the tasks based on their difficulties. We formalize these objectives in Section 4. The learnt embeddings are evaluated on the following application scenarios: (a) given the realizations of the optimality variables of a set of tasks for an agent θ , predict the most probable realization of the optimality variable of a new task for the same agent without observing θ , and (b) amongst several options of tasks $\mathcal{S}_{\text{options}}$, choose the task that best matches desired characteristics, such as selecting tasks that are slightly harder than a reference task.

4 Learning Framework

In Sections 4.1 and 4.2, we formally define our information-theoretic criterion to measure task similarity in reinforcement learning and describe an algorithm to empirically estimate it. In Section 4.3, we view the problem of learning task embeddings through the lens of ordinal constraint satisfaction.

4.1 Information-Theoretic Measure of Task Similarity

Our goal is to measure similarity between sequential tasks. To this end, we propose the mutual information between task optimality variables as a measure of task similarity. This metric captures the intuition that two tasks are similar to each other if observing an agent’s performance on one task reduces our uncertainty about its performance on the other. We begin by formally defining performance uncertainty. Thereafter, we provide a formal definition of our task similarity criterion.

Definition 1 (Performance Uncertainty). *The entropy of the population with prior $p(\theta)$ solving a task s is defined as:*

$$\mathcal{H}(\mathcal{O}_{s,\Theta}) = - \sum_{o \in \{0,1\}} P(\mathcal{O}_{s,\Theta} = o) \log P(\mathcal{O}_{s,\Theta} = o),$$

where $\mathcal{O}_{s,\Theta}$ is the optimality variable for s .

Thus, we could measure the similarity between two tasks $s_i, s_j \in \mathcal{S}_{\text{init}}$ as the reduction in $\mathcal{H}(\mathcal{O}_{s_i,\Theta})$ by observing $\mathcal{O}_{s_j,\Theta}$.

Definition 2 (Task Similarity). *Given a prior over the population of agents $p(\theta)$, we measure the similarity between two tasks $s_i, s_j \in \mathcal{S}_{\text{init}}$ as the mutual information $\mathcal{I}(\cdot; \cdot)$ between their optimality variables $\mathcal{O}_{s_i,\Theta}, \mathcal{O}_{s_j,\Theta}$:*

$$\mathcal{I}(\mathcal{O}_{s_i,\Theta}; \mathcal{O}_{s_j,\Theta}) = \mathcal{H}(\mathcal{O}_{s_i,\Theta}) - \mathcal{H}(\mathcal{O}_{s_i,\Theta} \mid \mathcal{O}_{s_j,\Theta}).$$

It quantifies the information obtained about $\mathcal{O}_{s_i,\Theta}$ by observing $\mathcal{O}_{s_j,\Theta}$.

4.2 Empirical Estimation of \mathcal{I}

We now describe an algorithm to empirically estimate \mathcal{I} . The pseudocode for the proposed algorithm is provided in the Appendix. Given an MDP \mathcal{M} and a prior distribution of the agent parameters $p(\theta)$, our algorithm uses N samples to estimate $\mathcal{I}(\mathcal{O}_{s_i,\Theta}; \mathcal{O}_{s_j,\Theta})$. For each sample, the algorithm randomly samples $\theta_l \sim p(\theta)$, and performs rollouts of π_{θ_l} from s_i and s_j to obtain estimates of the probability mass functions required for the computation of \mathcal{I} . The estimation procedure can be invoked with the signature $\text{ESTIMATE}(s_i, s_j, \mathcal{M}, \pi, p(\theta), N)$.

4.3 Learning Task Embeddings

With the criterion to measure task similarity defined, we are interested in learning a task embedding function

$f_\phi : \mathcal{S}_{\text{init}} \rightarrow \mathbb{R}^n$ (consequently, an embedding space) that meets the requirements introduced in Section 3. To this end, we pose the problem of learning $f_\phi(\cdot)$ as an ordinal constraint satisfaction problem. Essentially, the task similarity criterion \mathcal{I} imposes a set \mathcal{C}_{MI} of triplet ordinal constraints on the task embeddings. $\text{POS}(\cdot)$ imposes another set $\mathcal{C}_{\text{NORM}}$ of pairwise ordinal constraints.

Concretely, \mathcal{C}_{MI} is a collection of ordered triplets of tasks s.t. for each $(s_1, s_2, s_3) \in \mathcal{C}_{\text{MI}}$, $\mathcal{I}(\mathcal{O}_{s_1,\Theta}; \mathcal{O}_{s_2,\Theta}) > \mathcal{I}(\mathcal{O}_{s_1,\Theta}; \mathcal{O}_{s_3,\Theta})$. Consequently, we would like to satisfy the constraint $\langle f_\phi(s_1), f_\phi(s_2) \rangle > \langle f_\phi(s_1), f_\phi(s_3) \rangle$. Likewise, $\mathcal{C}_{\text{NORM}}$ is a collection of ordered tuples of tasks s.t. for each $(s_1, s_2) \in \mathcal{C}_{\text{NORM}}$, $\text{POS}(s_1) > \text{POS}(s_2)$. Consequently, we would like to satisfy the constraint $\|f_\phi(s_2)\|_2 > \|f_\phi(s_1)\|_2$ (embeddings for easier tasks have smaller norm).

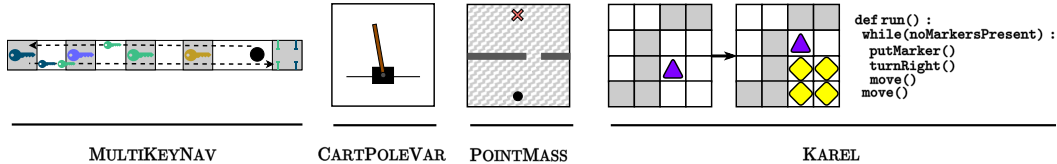
We learn the task embedding function $f_\phi(s)$, for an MDP \mathcal{M} and a prior over the population of agents $p(\theta)$, by optimizing the parameters ϕ to maximize the log-likelihood of the ordinal constraints under

Algorithm 1 Learn the Task Embedding Function (f_ϕ)

- 1: **procedure** TRAIN(Set of tasks $\mathcal{S}_{\text{init}}$, MDP \mathcal{M} , Policy π , Prior distribution of the agent parameters $p(\theta)$, Number of samples N , Hyperparameter λ , Number of iterations M)
 - 2: Initialize ϕ .
 - 3: **for** $i \in \{1, \dots, M\}$ **do**
 - 4: Sample task $s_1, s_2, s_3 \sim \mathcal{S}_{\text{init}}$.
 - 5: $E_1, E_2, E_3 \leftarrow f_\phi(s_1), f_\phi(s_2), f_\phi(s_3)$
 - 6: $\hat{\mathcal{I}}_{12} \leftarrow \text{ESTIMATE}(s_1, s_2, \mathcal{M}, \pi, p(\theta), N)$
 - 7: $\hat{\mathcal{I}}_{13} \leftarrow \text{ESTIMATE}(s_1, s_3, \mathcal{M}, \pi, p(\theta), N)$
 - 8: **if** $\hat{\mathcal{I}}_{12} > \hat{\mathcal{I}}_{13}$ **then**
 - 9: loss $\leftarrow \log(1 + \exp(\langle E_1, E_3 \rangle - \langle E_1, E_2 \rangle))$
 - 10: **else**
 - 11: loss $\leftarrow \log(1 + \exp(\langle E_1, E_2 \rangle - \langle E_1, E_3 \rangle))$
 - 12: Sample task $s_4, s_5 \sim \mathcal{S}_{\text{init}}$.
 - 13: $E_4, E_5 \leftarrow f_\phi(s_4), f_\phi(s_5)$
 - 14: **if** $\text{POS}(s_4) > \text{POS}(s_5)$ **then**
 - 15: loss $\leftarrow \text{loss} + \lambda \log(1 + \exp(\|E_4\|_2 - \|E_5\|_2))$
 - 16: **else**
 - 17: loss $\leftarrow \text{loss} + \lambda \log(1 + \exp(\|E_5\|_2 - \|E_4\|_2))$
 - 18: Update ϕ to minimize loss.
 - 19: **return** ϕ
-

Environment	Task Variability	Action	State	Number of Tasks
MULTIKEYNAV	Reward Function	7	$\mathbb{R} \times \{0, 1\}^6$	Infinite
CARTPOLEVAR	Dynamics	2	$\mathbb{R}^5 \times \{0, 1\} \times [200]$	Infinite
POINTMASS	Dynamics	\mathbb{R}^2	\mathbb{R}^7	Infinite
KAREL	Reward Function + Dynamics	52	$\{0, 1\}^{51840}$	73688
BASICKAREL	Reward Function + Dynamics	6	$\{0, 1\}^{88}$	24000

(a) Comparison of environments' complexity



(b) Illustrations

Figure 2: We evaluate our framework on a diverse set of environments. (a) compares the characteristics of these environments. (b) illustrates these environments for a better understanding of the tasks.

the Bradley-Terry-Luce (BTL) model [38]. Concretely, given a triplet of tasks (s_1, s_2, s_3) , we define:

$$P((s_1, s_2, s_3) \in \mathcal{C}_{\text{MI}}) := \frac{\exp(\langle f_\phi(s_1), f_\phi(s_2) \rangle)}{\exp(\langle f_\phi(s_1), f_\phi(s_2) \rangle) + \exp(\langle f_\phi(s_1), f_\phi(s_3) \rangle)}.$$

Similarly, given a tuple of tasks (s_1, s_2) , we define:

$$P((s_1, s_2) \in \mathcal{C}_{\text{NORM}}) := \frac{\exp(\|f_\phi(s_2)\|_2)}{\exp(\|f_\phi(s_1)\|_2) + \exp(\|f_\phi(s_2)\|_2)}.$$

Therefore, the task embedding function $f_\phi(s)$ is learnt by solving the following optimization problem:

$$\min_{\phi} \left[\mathbb{E}_{(s_1, s_2, s_3) \sim \mathcal{C}_{\text{MI}}} \log \left(1 + \exp(\langle E_1, E_3 \rangle - \langle E_1, E_2 \rangle) \right) + \lambda \mathbb{E}_{(s_4, s_5) \sim \mathcal{C}_{\text{NORM}}} \log \left(1 + \exp(\|E_4\|_2 - \|E_5\|_2) \right) \right],$$

where E_i denotes $f_\phi(s_i)$, and λ is a hyperparameter. The pseudocode for the proposed algorithm to learn the task embedding function $f_\phi(\cdot)$ is given in Algorithm 1.

5 Experiments: Visualization of Embedding Spaces

In this section, we visualize the embedding spaces to gather qualitative insights. Specifically, we seek to answer the following research questions: (i) Can distinct clusters of tasks be identified by visualizing the embedding space on a 2-dimensional map using t-SNE [39]? (ii) How does regularization through $\mathcal{C}_{\text{NORM}}$ affect the embedding space? (iii) What is the effect of agent population and environment specification on the embedding space? We begin by discussing the rationale for environment selection, and then describe the environments used for the evaluation. Subsequently, we provide an overview of the embedding networks' training process, followed by the qualitative results.

5.1 Environments

We evaluate our framework on environments with diverse characteristics to demonstrate its generality and scalability to different sequential decision-making problems. In this work, we use MULTIKEYNAV as the running example because it is compositional (the agent needs to compose different actions for picking keys in a task-specific manner to unlock the door), which also makes it suitable for ablation experiments. Considering that task variability in MULTIKEYNAV comes from the reward function, we use CARTPOLEVAR to highlight our framework's applicability to environments in which task variability comes from the dynamics instead. We select POINTMASS to test if our framework can handle continuous action spaces. Finally, to investigate our framework's scalability, we use the

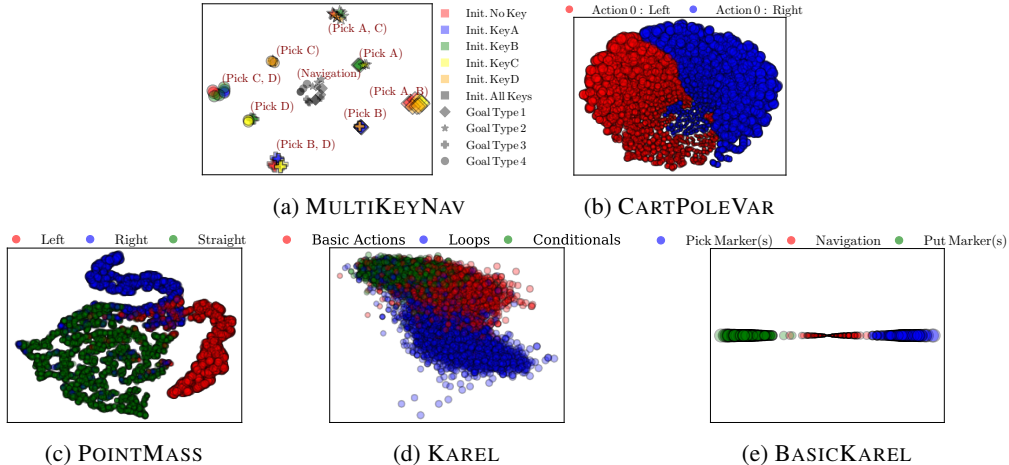


Figure 3: Visualization of the task embedding spaces learnt through our framework. Each point represents a task, and the size of the points is proportional to the norm of the embeddings.

real-world environment KAREL, which is a challenging environment with applications in programming education. In addition, we evaluate our framework on BASICKAREL, which is a simpler version of KAREL. Additional comparisons of the environments are presented in Figure 2.

MULTIKEYNAV. This environment corresponds to a navigation task in a one-dimensional line segment, where the agent has to pick certain keys using appropriate `pickKey` actions (one action for each key type) and unlock the door located towards the right. A task in this environment is considered to be solved if the agent successfully unlocks the door. The environment used in our experiments is based on the work of [40]; however, we adapted it to have multiple keys that need to be picked. More concretely, there are four keys, KeyA, KeyB, KeyC, and KeyD, located on different segments. Task variability in this environment comes from the agent’s initial position, the keys that it possesses initially, and the door type (with each type requiring a unique set of keys). In the ablation study, we will check the impact of changing the key requirements for the doors.

CARTPOLEVAR. This environment is a variation of the classic control task from OpenAI gym [41], and also takes inspiration from [42] in which the forces applied by each action could be negative as well. More concretely, the environment consists of a pole attached to an unactuated joint to a cart, which moves along a track. The agent controls the cart in the presence of gravity by applying forces to the left (action 0) or to the right (action 1) of the cart. A task in this environment is considered to be solved if the agent keeps the pole upright for 200 timesteps. Task variability in this environment comes from the force $F \in [-15\text{ N}, -5\text{ N}] \cup [5\text{ N}, 15\text{ N}]$ applied on the cart by each action, and the $\text{TaskType} \in \{0, 1\}$. Tasks of Type 0 involve “Pulling” with action 0 pulling the cart from the left and action 1 pulling the cart from the right, while tasks of Type 1 involve “Pushing”.

POINTMASS. This environment was introduced in [43]. The agent applies forces to control a point mass inside a square surrounded by walls. Additionally, there is a gate of certain width at a certain position. A task in this environment is considered to be solved if the point mass reaches the fixed goal position, which requires crossing the gate. Task variability in this environment comes from the width w_g and the position p_g of the gate, along with the coefficient of kinetic friction μ_k of the space.

KAREL and BASICKAREL. This is the Karel program synthesis environment from [44]. Karel is an educational programming language which has been widely used in introductory CS courses. The environment consists of an agent inside a grid in which each cell could contain marker(s), correspond to a wall, or be empty. The agent can move inside the grid and modify it by picking or placing markers. The objective of each task is to synthesize the program π^* (one could think of this as a controller for the agent) in the Karel domain-specific language (DSL) given 5 input-output examples for it in the form of Pre-Grid and its corresponding Post-Grid. The synthesized program π could contain complex programming constructs like loops and conditionals. A task is considered to be solved if π generalizes to a held-out test example for π^* . Task variability in this environment comes from the set of input-output examples. BASICKAREL [45] is a variant of KAREL that excludes programming constructs like loops and conditionals, and only includes basic actions.

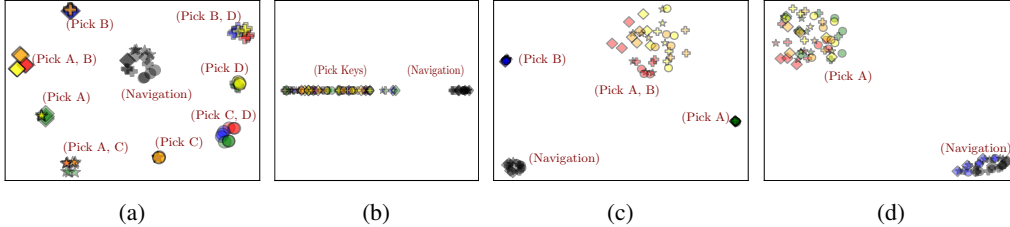


Figure 4: Task embedding spaces for the MULTIKEYNAV environment: (a) without C_{NORM} , (b) pickKey actions masked, (c) all doors require KeyA, KeyB, and (d) all doors require KeyA.

5.2 Training Process

We now describe the training process to learn the task embedding function. First, we obtain the agent population by taking snapshots while training a neural network policy using either behavioral cloning [46] or policy gradient methods [47]. Concretely, a snapshot is recorded if the average performance on a validation set of tasks (denoted as S_{snap}) improves by δ_{snap} compared to the previously recorded snapshot. A snapshot of the untrained policy is recorded by default. Different subpopulations, obtained by either masking actions or by using biased task distributions during training, are combined to form the final population. Here, masking a certain action corresponds to setting its logit to a large negative number. For behavioral cloning, action masking is equivalent to removing examples for the masked actions. Using biased task distribution during training is another way to inject diversity into the population. For the MULTIKEYNAV environment, for example, using a biased task distribution could correspond to assigning low probability mass to tasks with certain types of doors in the initial state distribution during training. Finally, we learn a task embedding function $f_{\phi}(\cdot)$ modelled by a neural network, the parameters of which are optimized as described in Algorithm 1.

5.3 Visualizations and Qualitative Results

We visualize the embedding spaces on a 2-dimensional map using t-SNE [39] to identify distinct clusters of tasks. Although t-SNE preserves the local structure, it does not necessarily preserve the embeddings’ norm. For this reason, we scale the points in proportion to the norm of the embeddings.

Visualizations. For the MULTIKEYNAV environment (Fig. 3a), our framework discovers distinct clusters of tasks, with each cluster corresponding to a unique set of keys that need to be picked. The norm of the embeddings is in accordance with the number of keys that need to be picked (with tasks requiring navigation only having the smallest norm). Additionally, tasks in clusters adjacent to each other share a common key requirement. For the CARPOLEVAR environment (Fig. 3b), our framework discovers that each task exhibits one of two types of underlying dynamics. In one (+ve F and Type 0, or -ve F and Type 1), action 0 moves the cart to the left, while in the other (-ve F and Type 0, or +ve F and Type 1), action 0 moves the cart to the right. For the POINTMASS environment (Fig. 3c), our framework discovers three clusters of tasks based on the behavior that the agent needs to exhibit near the gate. The first cluster include tasks in which the agent does not need to steer to cross the gate, while the second and third clusters contain tasks in which the agent must steer left or right to cross the gate, respectively. For the KAREL and BASICKAREL environments (Fig. 3d and 3e), our framework discovers different clusters of tasks based on whether the solution code requires loops or conditionals, and whether the agent needs to pick or put markers in the grid, respectively.

Ablation w.r.t. C_{NORM} . Fig. 4a shows the task embedding space learnt without the norm ordinal constraints C_{NORM} (i.e., λ is set to 0). As expected, the norm of the embeddings is not proportional to the number of keys that need to be picked. Instead, the points are nearly uniform in size.

Ablation w.r.t. population specification. To understand the effect of population on the task embedding space, we learn the embedding function $f_{\phi}(\cdot)$ for the MULTIKEYNAV environment using an agent population in which pickKey actions are masked (Fig. 4b). In this case, we obtain two distinct clusters of tasks – one of the clusters contains tasks that cannot be solved (these tasks require picking key(s)), and the other contains tasks that require navigation only. These results emphasize the importance of the population’s quality in learning a good task embedding space.

Ablation w.r.t. environment specification. In this ablation experiment, we change the environment specification and check its impact on the task embedding space. Concretely, we learn the embedding

space for the following variants of the MULTIKEYNAV environment: (a) each door requires KeyA and KeyB (Fig. 4c), i.e., all the doors have identical key requirements, and (b) each door requires KeyA only (Fig. 4d). Modifying the environment specification changes the task semantics, thereby impacting the task embedding space. Thus, these results are inline with our intuition.

6 Experiments: Application Scenarios

In this section, we evaluate our framework on two application scenarios: performance prediction, and task selection. We conduct this evaluation on the MULTIKEYNAV and CARTPOLEVAR environments as they cover two distinct sources of task variability, namely reward function and dynamics.

6.1 Performance Prediction

First, we assess the quality of the learnt task embeddings by using them to predict an agent’s performance on a task $s_{\text{test}} \in \mathcal{S}_{\text{init}}$ after observing its performance on a quiz $\mathcal{S}_{\text{quiz}} \subseteq \mathcal{S}_{\text{init}}$. Specifically, through experiments, we seek to answer the following research question: Would an agent show similar performance on tasks that lie close to each other in the learnt task embedding space? We begin by designing a benchmark for this application scenario, and then compare our technique for performance prediction using task embeddings against several baselines.

Benchmark. Formally, given the realizations of the task optimality variables of a set of tasks for an agent θ , we are interested in predicting the most probable realization of the task optimality variable of a new task for the same agent without observing θ . To build benchmarks for this scenario, we generate datasets for all quiz sizes ranging from 1 to 20, each with 5000 examples for training and 5000 examples for testing. Each example is generated by randomly sampling a quiz $\mathcal{S}_{\text{quiz}}$ of desired size, along with a task s_{test} from $\mathcal{S}_{\text{init}}$, and then recording the performance of an agent θ , sampled from the population, on these tasks. Performance prediction techniques are evaluated on this benchmark by measuring the prediction accuracy on the test examples in the dataset. The techniques are evaluated on each dataset by partitioning it into 10 folds and reporting the mean prediction accuracy across the folds along with the standard error.

Our approach. Our prediction technique performs soft-nearest neighbor matching of s_{test} with $\mathcal{S}_{\text{quiz}}$ in the task embedding space to predict performance on s_{test} . Concretely, given the embedding function $f_\phi(\cdot)$, the prediction is $\mathbb{1}_{c>0.5}$, where c equals $\frac{\sum_{s \in \mathcal{S}_{\text{quiz}}} o_s \exp(-\beta \|f_\phi(s) - f_\phi(s_{\text{test}})\|_2^2)}{\sum_{s \in \mathcal{S}_{\text{quiz}}} \exp(-\beta \|f_\phi(s) - f_\phi(s_{\text{test}})\|_2^2)}$, o_s is the realization of the task optimality variable for task s , and β is a hyperparameter.

Baselines. We compare our technique against the following baselines: (i) *Random*: The agent’s performance on s_{test} is predicted randomly. (ii) *IgnoreTask*: The agent is predicted to succeed on s_{test} iff the probability that it succeeds on a random task is more than 0.5. (iii) *IgnoreAgent*: The agent is predicted to succeed on s_{test} iff the probability that a random agent succeeds on s_{test} is more than 0.5. (iv) *OPT*: The agent is predicted to succeed on s_{test} iff the probability that it succeeds on s_{test} is more than 0.5.

Results. Figure 5 shows the prediction accuracies of different techniques on the performance prediction benchmarks. It is evident that our technique is competitive with the *OPT* baseline, which provides an upper-bound on the prediction accuracy. Note that *OPT* is an unrealistic technique since it assumes that both the agent and the task can be observed.

6.2 Tasks Selection

Next, we assess the learnt embeddings by using them to select tasks with desired characteristics. Specifically, we seek to answer the following research questions: (i) Does the inner product in the

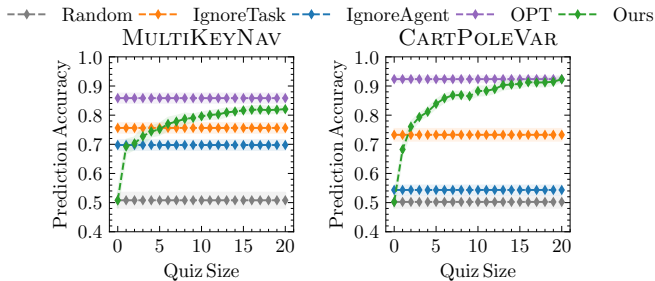


Figure 5: Results for performance prediction using task embeddings. Our technique (listed as *Ours*) is competitive with the *OPT* baseline, which is the best one could do on this benchmark.

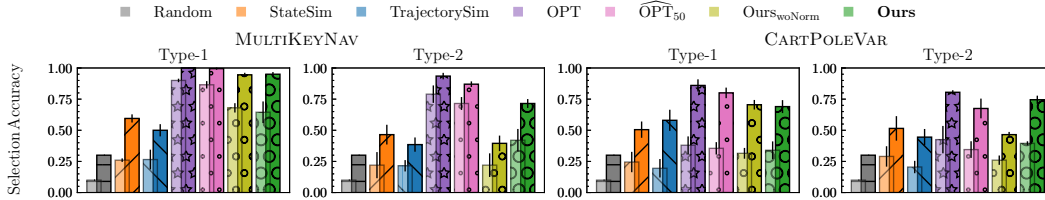


Figure 6: Results for task selection using task embeddings (dark bars represent Top-3 accuracy and light bars represent Top-1). Our technique (listed as *Ours*) is competitive with \widehat{OPT}_{50} . Further, it outperforms *Ours_{woNorm}* on Type-2 queries, highlighting the significance of \mathcal{C}_{NORM} in our framework.

learnt task embedding space capture task similarity based on our information-theoretic criterion? (ii) Does the norm of the embedding learnt by our framework induce an ordering on the tasks based on their difficulties? We begin by designing a benchmark for this application scenario, and then compare our technique for task selection using task embeddings against several baselines.

Benchmark. Amongst several options of tasks $\mathcal{S}_{options}$, we are interested in choosing the task that best matches the desired characteristics. We categorize the desired characteristics into two query types: *Type-1*: Select the task that is the most similar to a given reference task s_{ref} . The ground-truth answer to this query is $\arg \max_{s \in \mathcal{S}_{options}} \mathcal{I}(\mathcal{O}_{s_{ref}}, \Theta; \mathcal{O}_s, \Theta)$. *Type-2*: Select the task that is the most similar to (but harder than) a given reference task s_{ref} . Out of all the tasks in $\mathcal{S}_{options}$ that are harder than s_{ref} , the ground-truth answer to this query is the task most similar to it. To build benchmarks for this scenario, we generate a dataset of 50 examples, where each example is constructed by randomly sampling s_{ref} along with 10 tasks that form $\mathcal{S}_{options}$. In addition to these examples, each benchmark provides 5 easy tasks for reference (determined by ranking a randomly sampled pool of 500 tasks). Task selection techniques are evaluated by reporting the mean selection accuracy on 4 randomly sampled datasets along with the standard error.

Our approach. We use task embeddings to rank the options according to similarity and/or difficulty, based on which the selection is made. We additionally compare our technique based on task embeddings learnt without \mathcal{C}_{NORM} (listed as *Ours_{woNorm}*).

Baselines. Our technique is compared against the following baselines on the task selection benchmark: (i) *Random*: Answers to queries are randomly selected from $\mathcal{S}_{options}$. (ii) *StateSim*: Similarity between tasks is determined using the distance between the state representations. For queries of type 2, this technique considers a task s_1 to be harder than s_2 iff the similarity between s_1 and the task most similar to it in the set of easy reference tasks, is less than that for s_2 . (iii) *TrajectorySim*: Similarity between tasks is determined using the edit distance between the tasks’ expert trajectories. (iv) *OPT*: Task similarity and difficulty is estimated using the entire population of agents. Given the variance in the estimation process, this is the best one could do on this benchmark. (v) \widehat{OPT}_{50} : Task similarity and difficulty is estimated using a randomly sampled 50% of the population.

Results. Figure 6 compares the selection accuracies of different techniques on the task selection benchmark. Our technique outperforms *Random*, *StateSim*, and *TrajectorySim*, and is competitive with \widehat{OPT}_{50} . This indicates that the inner product in the learnt task embedding space successfully captures similarity between tasks. Compared to *Ours_{woNorm}*, our technique performs significantly better on Type-2 queries, which indicates that the norm of the embedding learnt by our framework induces an ordering on the tasks based on their difficulties.

7 Conclusion

In this work, we presented an information-theoretic framework to learn task embeddings in sequential decision-making settings. Through experiments on a diverse set of environments, we empirically demonstrated that the inner product in the embedding space captures similarity between tasks, and the norm of the embedding induces an ordering on the tasks based on their difficulties. One apparent limitation of our current framework is that it requires the tasks to be goal-based, which we plan to address in future work. Additionally, the agent population plays a crucial role in our framework, and therefore, it would be interesting to explore more principled methods for construction that explicitly

optimize for diversity in the population. Further, empirically estimating the proposed task similarity criterion by directly estimating the underlying mass functions could be sample-inefficient for some environments. Therefore, a promising direction for future work is to construct sample-efficient estimators for this criterion. Moreover, evaluation in multi-agent settings, where the task embedding could encode the behavior of non-ego agents, is another interesting direction for future work.

Acknowledgments and Disclosure of Funding

Funded/Co-funded by the European Union (ERC, TOPS, 101039090). Views and opinions expressed are however those of the author(s) only and do not necessarily reflect those of the European Union or the European Research Council. Neither the European Union nor the granting authority can be held responsible for them.

References

- [1] Yi Sun, Xiaogang Wang, and Xiaoou Tang. Deep Learning Face Representation from Predicting 10,000 Classes. In *CVPR*, 2014.
- [2] Flood Sung, Yongxin Yang, Li Zhang, Tao Xiang, Philip H. S. Torr, and Timothy M. Hospedales. Learning to Compare: Relation Network for Few-Shot Learning. In *CVPR*, 2018.
- [3] Ali Athar, Sabarinath Mahadevan, Aljoša Ošep, Laura Leal-Taixé, and Bastian Leibe. STEm-Seg: Spatio-temporal Embeddings for Instance Segmentation in Videos. In *ECCV*, 2020.
- [4] Tomas Mikolov, Ilya Sutskever, Kai Chen, Greg S Corrado, and Jeff Dean. Distributed Representations of Words and Phrases and their Compositionality. In *NIPS*, 2013.
- [5] Jeffrey Pennington, Richard Socher, and Christopher D. Manning. GloVe: Global Vectors for Word Representation. In *EMNLP*, 2014.
- [6] Daniel Matthew Cer, Yinfei Yang, Sheng yi Kong, Nan Hua, Nicole Limtiaco, Rhomni St. John, Noah Constant, Mario Guajardo-Cespedes, Steve Yuan, Chris Tar, Brian Strope, and Ray Kurzweil. Universal Sentence Encoder for English. In *EMNLP*, 2018.
- [7] Yu Zhang, Ying Wei, and Qiang Yang. Learning to Multitask. In *NeurIPS*, 2018.
- [8] Alessandro Achille, Michael Lam, Rahul Tewari, Avinash Ravichandran, Subhansu Maji, Charless C. Fowlkes, Stefano Soatto, and Pietro Perona. Task2Vec: Task Embedding for Meta-Learning. In *ICCV*, 2019.
- [9] Xingchao Peng, Yichen Li, and Kate Saenko. Domain2Vec: Domain Embedding for Unsupervised Domain Adaptation. In *ECCV*, 2020.
- [10] Rongjun Qin, F. Chen, Tonghan Wang, Lei Yuan, Xiaoran Wu, Zongzhang Zhang, Chongjie Zhang, and Yang Yu. Multi-Agent Policy Transfer via Task Relationship Modeling. *ArXiv*, 2022.
- [11] Lukas Schäfer, Filippos Christianos, Amos J. Storkey, and Stefano V. Albrecht. Learning Task Embeddings for Teamwork Adaptation in Multi-Agent Reinforcement Learning. *ArXiv*, 2022.
- [12] Isac Arnekvist, Danica Kragic, and Johannes Andreas Stork. VPE: Variational Policy Embedding for Transfer Reinforcement Learning. In *ICRA*, 2018.
- [13] Minjong Yoo, Sangwoo Cho, and Honguk Woo. Skills Regularized Task Decomposition for Multi-task Offline Reinforcement Learning. In *NeurIPS*, 2022.
- [14] Kate Rakelly, Aurick Zhou, Chelsea Finn, Sergey Levine, and Deirdre Quillen. Efficient Off-Policy Meta-Reinforcement Learning via Probabilistic Context Variables. In *ICML*, 2019.
- [15] Z. Bing, D. Lerch, K. Huang, and A. Knoll. Meta-Reinforcement Learning in Non-Stationary and Dynamic Environments. In *IEEE TPAMI*, 2023.
- [16] Abhishek Gupta, Russell Mendonca, YuXuan Liu, Pieter Abbeel, and Sergey Levine. Meta-Reinforcement Learning of Structured Exploration Strategies. In *NIPS*, 2018.
- [17] Haotian Fu, Hongyao Tang, Jianye Hao, Chen Chen, Xidong Feng, Dong Li, and Wulong Liu. Towards Effective Context for Meta-Reinforcement Learning: an Approach based on Contrastive Learning. In *AAAI*, 2020.

- [18] Lanqing Li, Rui Yang, and Dijun Luo. FOCAL: Efficient Fully-Offline Meta-Reinforcement Learning via Distance Metric Learning and Behavior Regularization. In *ICLR*, 2021.
- [19] Lin Lan, Zhenguo Li, Xiaohong Guan, and Pinghui Wang. Meta Reinforcement Learning with Task Embedding and Shared Policy. In *IJCAI*, 2019.
- [20] Homer Walke, Jonathan Yang, Albert Yu, Aviral Kumar, Jędrzej Orbik, Avi Singh, and Sergey Levine. Don't Start From Scratch: Leveraging Prior Data to Automate Robotic Reinforcement Learning. In *CoRL*, 2022.
- [21] Shagun Sodhani, Amy Zhang, and Joelle Pineau. Multi-Task Reinforcement Learning with Context-based Representations. In *ICML*, 2021.
- [22] Risto Vuorio, Shao-Hua Sun, Hexiang Hu, and Joseph J. Lim. Multimodal Model-Agnostic Meta-Learning via Task-Aware Modulation. In *NeurIPS*, 2019.
- [23] Tu Vu, Tong Wang, Tsendsuren Munkhdalai, Alessandro Sordani, Adam Trischler, Andrew Mattarella-Micke, Subhransu Maji, and Mohit Iyyer. Exploring and Predicting Transferability across NLP Tasks. In *EMNLP*, 2020.
- [24] Jacob Devlin, Ming-Wei Chang, Kenton Lee, and Kristina Toutanova. BERT: Pre-training of Deep Bidirectional Transformers for Language Understanding. In *NAACL-HLT*, 2019.
- [25] Xinran Liu, Yikun Bai, Yuzhe Lu, Andrea Soltoggio, and Soheil Kolouri. Wasserstein Task Embedding for Measuring Task Similarities. *ArXiv*, 2022.
- [26] Rishabh Agarwal, Marlos C. Machado, Pablo Samuel Castro, and Marc G Bellemare. Contrastive Behavioral Similarity Embeddings for Generalization in Reinforcement Learning. In *ICLR*, 2021.
- [27] Amy Zhang, Rowan Thomas McAllister, Roberto Calandra, Yarın Gal, and Sergey Levine. Learning Invariant Representations for Reinforcement Learning without Reconstruction. In *ICLR*, 2021.
- [28] Philippe Hansen-Estruch, Amy Zhang, Ashvin Nair, Patrick Yin, and Sergey Levine. Bisimulation Makes Analogies in Goal-Conditioned Reinforcement Learning. In *ICML*, 2022.
- [29] Karol Hausman, Jost Tobias Springenberg, Ziyu Wang, Nicolas Heess, and Martin Riedmiller. Learning an Embedding Space for Transferable Robot Skills. In *ICLR*, 2018.
- [30] Jack Parker-Holder, Aldo Pacchiano, Krzysztof M Choromanski, and Stephen J Roberts. Effective Diversity in Population Based Reinforcement Learning. In *NeurIPS*, 2020.
- [31] Denis Yarats, Rob Fergus, Alessandro Lazaric, and Lerrel Pinto. Reinforcement Learning with Prototypical Representations. In *ICML*, 2021.
- [32] Taewook Nam, Shao-Hua Sun, Karl Pertsch, Sung Ju Hwang, and Joseph J Lim. Skill-based Meta-Reinforcement Learning. In *ICLR*, 2022.
- [33] William Whitney, Rajat Agarwal, Kyunghyun Cho, and Abhinav Gupta. Dynamics-Aware Embeddings. In *ICLR*, 2020.
- [34] Hiroki Furuta, Tatsuya Matsushima, Tadashi Kozuno, Yutaka Matsuo, Sergey Levine, Ofir Nachum, and Shixiang Shane Gu. Policy Information Capacity: Information-Theoretic Measure for Task Complexity in Deep Reinforcement Learning. In *ICML*, 2021.
- [35] Paul Tylkin, Goran Radanovic, and David C. Parkes. Learning Robust Helpful Behaviors in Two-Player Cooperative Atari Environments. In *AAMAS*, 2021.
- [36] Oriol Vinyals and et al. Grandmaster Level in StarCraft II Using Multi-agent Reinforcement Learning. In *Nature*, 2019.
- [37] Max Jaderberg and et al. Human-level Performance in 3D Multiplayer Games with Population-based Reinforcement Learning. In *Science*, 2019.
- [38] R. Duncan Luce. *Individual Choice Behavior: A Theoretical analysis*. Wiley, 1959.
- [39] Laurens van der Maaten and Geoffrey Hinton. Visualizing Data using t-SNE. In *JMLR*, 2008.
- [40] Rati Devidze, Goran Radanovic, Parameswaran Kamalaruban, and Adish Singla. Explicable Reward Design for Reinforcement Learning Agents. In *NeurIPS*, 2021.
- [41] Greg Brockman, Vicki Cheung, Ludwig Pettersson, Jonas Schneider, John Schulman, Jie Tang, and Wojciech Zaremba. OpenAI Gym. *ArXiv*, 2016.

- [42] Shagun Sodhani, Ludovic Denoyer, Pierre-Alexandre Kamienny, and Olivier Delalleau. MTEnv - Environment interface for multi-task reinforcement learning. GitHub, 2021.
- [43] P. Klink, C. D’Eramo, J. Peters, and J. Pajarinen. Self-Paced Deep Reinforcement Learning. In *NeurIPS*, 2020.
- [44] Rudy Bunel, Matthew J. Hausknecht, Jacob Devlin, Rishabh Singh, and Pushmeet Kohli. Leveraging Grammar and Reinforcement Learning for Neural Program Synthesis. In *ICLR*, 2018.
- [45] Georgios Tzannetos, Bárbara Gomes Ribeiro, Parameswaran Kamalaruban, and Adish Singla. Proximal Curriculum for Reinforcement Learning Agents. In *TMLR*, 2023.
- [46] Michael Bain and Claude Sammut. A Framework for Behavioural Cloning. In *Machine Intelligence, Intelligent Agents*, 1995.
- [47] Richard S Sutton, David McAllester, Satinder Singh, and Yishay Mansour. Policy Gradient Methods for Reinforcement Learning with Function Approximation. In *NIPS*, 1999.

A Table of Contents

In this section, we briefly describe the content provided in the paper’s appendices.

- Appendix B discusses the broader impact of the work and the compute resources required.
- Appendix C provides detailed descriptions of the environments used for experimental evaluation.
- Appendix D provides additional implementation details for experimental evaluation.
- Appendix E provides annotated visualization of the task embedding spaces.
- Appendix F provides additional results examining the embedding function’s generalization ability.
- Appendix G provides the pseudocode for our algorithm to empirically estimate \mathcal{I} .

B Discussion

Broader impact. Our work is algorithmic in nature and we do not see any direct societal implications.

Compute resources. All the experiments were conducted on a cluster of machines with Intel Xeon Gold 6134M CPUs (clocked at 3.20 Ghz) and Nvidia Tesla V100 GPUs (32 GB VRAM configuration). We would like to highlight that learning the task embedding function is a one-time process, which could be compute intensive. However, once the training is completed, computing the embeddings or utilizing them to measure task similarity is a one-shot operation.

C Environment Details

Below we provide detailed descriptions of the environments.

C.1 MULTIKEYNAV

This environment corresponds to a navigation task in a one-dimensional line segment $[0, 1]$, where the agent has to pick certain keys using appropriate `pickKey` actions (one action for each key type) and unlock the door located towards the right. A task in this environment is considered to be solved if the agent successfully unlocks the door. The environment used in our experiments is based on the work of [40]; however, we adapted it to have multiple keys that need to be picked.

More concretely, there are four keys, `KeyA`, `KeyB`, `KeyC`, and `KeyD`, located on the segments $[0, 0.1]$, $[0.2, 0.3]$, $[0.4, 0.5]$, $[0.6, 0.7]$, respectively. A door is located on the segment $[0.9, 1]$. The door could be of the following 4 types: Type 1 (00), Type 2 (01), Type 3 (10), or Type 4 (11). Doors of Type 1 require `KeyA` and `KeyB`, doors of Type 2 require `KeyA` and `KeyC`, doors of Type 3 require `KeyB` and `KeyD`, and doors of Type 4 require `KeyC` and `KeyD`.

The set of initial states, $\mathcal{S}_{\text{init}}$, is the same as the set of states \mathcal{S} . Each state $s \in \mathcal{S}$ corresponds to a 7-tuple (Location, `KeyStatusA`, `KeyStatusB`, `KeyStatusC`, `KeyStatusD`, `doorBit1`, `doorBit2`). Here, Location denotes the agent’s location on the line segment, and `KeyStatusA`, `KeyStatusB`, `KeyStatusC`, `KeyStatusD` are flags for whether the agent has picked up the corresponding key. Task variability in this environment comes from the agent’s initial position, the keys that it possesses initially, and the door type (with each type requiring a unique set of keys).

The action space is $\mathcal{A} = \{\text{moveLeft}, \text{moveRight}, \text{pickKeyA}, \text{pickKeyB}, \text{pickKeyC}, \text{pickKeyD}, \text{finish}\}$. `moveLeft` and `moveRight` move the agent across the environment with step size $0.075 + \epsilon$, where $\epsilon \sim U(-0.01, 0.01)$. If `pickKeyA` is executed at a location that lies on the segment containing `KeyA`, `KeyStatusA` becomes `True`, else the environment crashes. Likewise for `pickKeyB`, `pickKeyC`, and `pickKeyD`. The agent gets a reward of 1 on executing `finish` if it is at a location that lies on the segment containing the door and possesses the required keys; `finish` results in a crash otherwise. The horizon length is 40 and γ is 0.999.

C.2 CARTPOLEVAR

This environment is a variation of the classic control task from OpenAI gym [41], and also takes inspiration from [42] in which the forces applied by each action could be negative as well. It consists

of a pole (mass: 0.1 kg, length: 1 m) attached by an unactuated joint to a cart (mass: 1 kg), which moves along a track. The agent controls the cart in the presence of gravity ($g: 9.8 \text{ m/s}^2$) by applying forces to the left (action 0) or to the right (action 1) of the cart. A task in this environment is considered to be solved if the agent keeps the pole upright for 200 timesteps.

Each state $s \in \mathcal{S}$ corresponds to a tuple $(x, v, \theta, \omega, F, \text{TaskType}, \text{NumSteps})$. Here, x denotes the position of the cart, v denotes the velocity of the cart, θ denotes the angle that the pole makes with the vertical, ω denotes the angular velocity of the pole, $F \in [-15 \text{ N}, -5 \text{ N}] \cup [5 \text{ N}, 15 \text{ N}]$ denotes the force applied on the cart by each action, $\text{TaskType} \in \{0, 1\}$ denotes the type of the task, and NumSteps denotes the number of steps passed since the beginning of the episode. The action space is $\mathcal{A} = \{0, 1\}$.

Task variability in this environment comes from the force F applied on the cart by each action, and the $\text{TaskType} \in \{0, 1\}$. Tasks of Type 0 involve “Pulling” with action 0 pulling the cart from the left and action 1 pulling the cart from the right, while tasks of Type 1 involve “Pushing”. At any timestep, if $\theta \notin [-12^\circ, 12^\circ]$, the pole is not upright and consequently, the environment crashes. The horizon length is 200 and γ is 1.

C.3 POINTMASS

This environment was introduced in [43]. We provide the details here for the sake of completeness.

The agent applies forces to control a point mass inside a square space $[-4, 4] \times [-4, 4]$ surrounded by walls. The space exhibits friction, with the coefficient of kinetic friction $\mu_k \in [0, 4]$. Additionally, there is a gate of width $w_g \in [-4, 4]$ at position $p_g \in [0.5, 8]$, effectively spanning the segment $[p_g - 0.5w_g, p_g + 0.5w_g]$. The agent always starts off from the fixed initial position $[0, 3]$. A task in this environment is considered to be solved if the point mass reaches the fixed goal position $[0, -3]$, which requires crossing the gate.

Each state $s \in \mathcal{S}$ corresponds to a tuple (x, v_x, y, v_y) . Here, $[x, y]$ denotes the position of the point mass, while $[v_x, v_y]$ denotes the velocity. The actions are $[F_x, F_y] \in [-10, 10] \times [-10, 10]$, where F_x and F_y correspond to forces applied along the x and the y axis, respectively. Task variability in this environment comes from the width w_g and the position p_g of the gate, along with the coefficient of kinetic friction μ_k of the space. At any timestep, if the point mass crashes into the wall, the environment crashes. The horizon length is 100 and γ is 0.99.

C.4 KAREL

This is the Karel program synthesis environment from [44]. Karel is an educational programming language which has been widely used in introductory CS courses. The environment consists of an agent (characterized by its position and orientation) inside an 18×18 grid in which each cell could contain up to 10 markers, correspond to a wall, or be empty. The agent can move inside the grid and modify it by picking or placing markers. The objective of each task is to synthesize the program π^* (which is a controller for the agent) in the Karel domain-specific language (DSL) given 5 input-output examples for it in the form of Pre-Grid and its corresponding Post-Grid. A task is considered to be solved if the synthesized program π generalizes to a held-out test example for π^* .

The Karel DSL is shown in Figure 7. Task variability in this environment comes from the set of input-output examples. The state in this environment comprises of the program specification (i.e., the input-output examples) and the partial program synthesized so far. The tokens of the DSL form the action space. The horizon length is 24 and γ is 1. We use a set of 73688 tasks (with the number of tokens in π^* ranging between 10 and 14) sampled from the dataset used in [44] (accessible at <https://msr-redmond.github.io/karel-dataset/>).

C.5 BASICKAREL

This environment, introduced in [45], is a variant of KAREL that excludes programming constructs like loops and conditionals, and only includes basic actions. We provide the details here for completeness.

The environment consists of an agent inside a 4×4 grid. Each cell in the grid could contain a marker, correspond to a wall, or be empty. The objective of each task is to generate a sequence of actions that transforms a pre-grid to a post-grid. The BASICKAREL dataset has 24000 training tasks and

```

Prog  $p$  := def run() :  $s$ 
Stmt  $s$  := while( $b$ ) :  $s$  | repeat( $r$ ) :  $s$  |  $s_1$ ;  $s_2$  |  $a$ 
      | if( $b$ ) :  $s$  | ifelse( $b$ ) :  $s_1$  else :  $s_2$ 
Cond  $b$  := frontIsClear() | leftIsClear() | rightIsClear()
      | markersPresent() | noMarkersPresent() | not  $b$ 
Action  $a$  := move() | turnRight() | turnLeft()
      | pickMarker() | putMarker()
Cste  $r$  := 0 | 1 |  $\dots$  | 19

```

Figure 7: The Karel domain-specific language (DSL) [44].

2400 validation tasks. The set of initial states, $\mathcal{S}_{\text{init}}$, is the same as the training set of tasks provided in the BASICKAREL dataset. Each state $s \in \mathcal{S}$ corresponds to a tuple (Curr-Grid, Post-Grid), where Curr-Grid and Post-Grid correspond to the bitmap representation of the current-grid and the post-grid, respectively.

The action space is $\mathcal{A} = \{\text{move}, \text{turnLeft}, \text{turnRight}, \text{pickMarker}, \text{putMarker}, \text{finish}\}$. `move` moves the agent in the facing direction. `turnLeft` and `turnRight` turn the agent left and right, respectively. The agent can pick and put a marker using `pickMarker` and `putMarker`, respectively. The agent gets a reward of 1 on executing `finish` if Curr-Grid matches Post-Grid (i.e., it has successfully transformed the pre-grid to the post-grid); `finish` results in a crash otherwise. The horizon length is 20 and γ is 0.999.

D Implementation Details

Training process. For all the environments, we set δ_{snap} to 0.01 (0.1 for KAREL) in our experiments. The average performance on $\mathcal{S}_{\text{snap}}$ is determined by performing 10 rollouts on each task in the set. We implement each embedding network using a succession of several fully connected layers with ReLU activations, trained for 300 epochs (500 epochs for CARTPOLEVAR and 10 epochs for KAREL) using the Adam optimizer with $1e - 3$ ($1e - 4$ for KAREL) learning rate, and batch size 128 (512 for KAREL). We sample 5000 (80000 for KAREL and 10000 for BASICKAREL) constraints from \mathcal{C}_{MI} and $\mathcal{C}_{\text{NORM}}$ each to train the network, the \hat{T} values of which are approximated using 100 samples from each agent in the population. `p_success(.)` is approximated using 10 samples from each agent in the population. The hyperparameters β and λ are set to 1000 and 0.4, respectively. In addition, we use a validation set and a test set, consisting of 1000 (16000 for KAREL and 2000 for BASICKAREL) constraints from \mathcal{C}_{MI} and $\mathcal{C}_{\text{NORM}}$ each, for early stopping and to determine the final model parameters. We vary the embedding dimensionality from 1 to 10 and choose the one after which the test loss does not decrease much. Below we provide environment-specific details:

- **MULTIKEYNAV:** For this environment, $\mathcal{S}_{\text{snap}}$ includes all combinations of the locations $\{0.05, 0.45, 0.85\}$, key statuses, and door types. We combine the subpopulations obtained by masking no action, masking each `pickKey` action individually, and masking all `pickKey` actions, to obtain an agent population of size 100. The embedding network has two hidden layers (32 neurons in each layer). The embedding dimensionality is 5 without $\mathcal{C}_{\text{NORM}}$, and 6 with $\mathcal{C}_{\text{NORM}}$.
- **CARTPOLEVAR:** For this environment, $\mathcal{S}_{\text{snap}}$ consists of 1000 tasks sampled from $\mathcal{S}_{\text{init}}$. We combine the subpopulations obtained by using all the tasks in $\mathcal{S}_{\text{init}}$, tasks in $\mathcal{S}_{\text{init}}$ with positive force and Type 0, tasks in $\mathcal{S}_{\text{init}}$ with positive force and Type 1, tasks in $\mathcal{S}_{\text{init}}$ with negative force and Type 0, and tasks in $\mathcal{S}_{\text{init}}$ with negative force and Type 1, to obtain an agent population of size 95. The embedding network has two hidden layers (64 neurons in the first layer and 32 neurons in the second). The embedding dimensionality is 2 without $\mathcal{C}_{\text{NORM}}$, and 3 with $\mathcal{C}_{\text{NORM}}$.
- **POINTMASS:** For this environment, $\mathcal{S}_{\text{snap}}$ consists of 100 tasks sampled from $\mathcal{S}_{\text{init}}$. We combine subpopulations obtained by using all the tasks in $\mathcal{S}_{\text{init}}$, tasks in $\mathcal{S}_{\text{init}}$ that satisfy the condition $p_g + 0.5w_g < 0$, and tasks in $\mathcal{S}_{\text{init}}$ that satisfy the condition $p_g + 0.5w_g \geq 0$, to

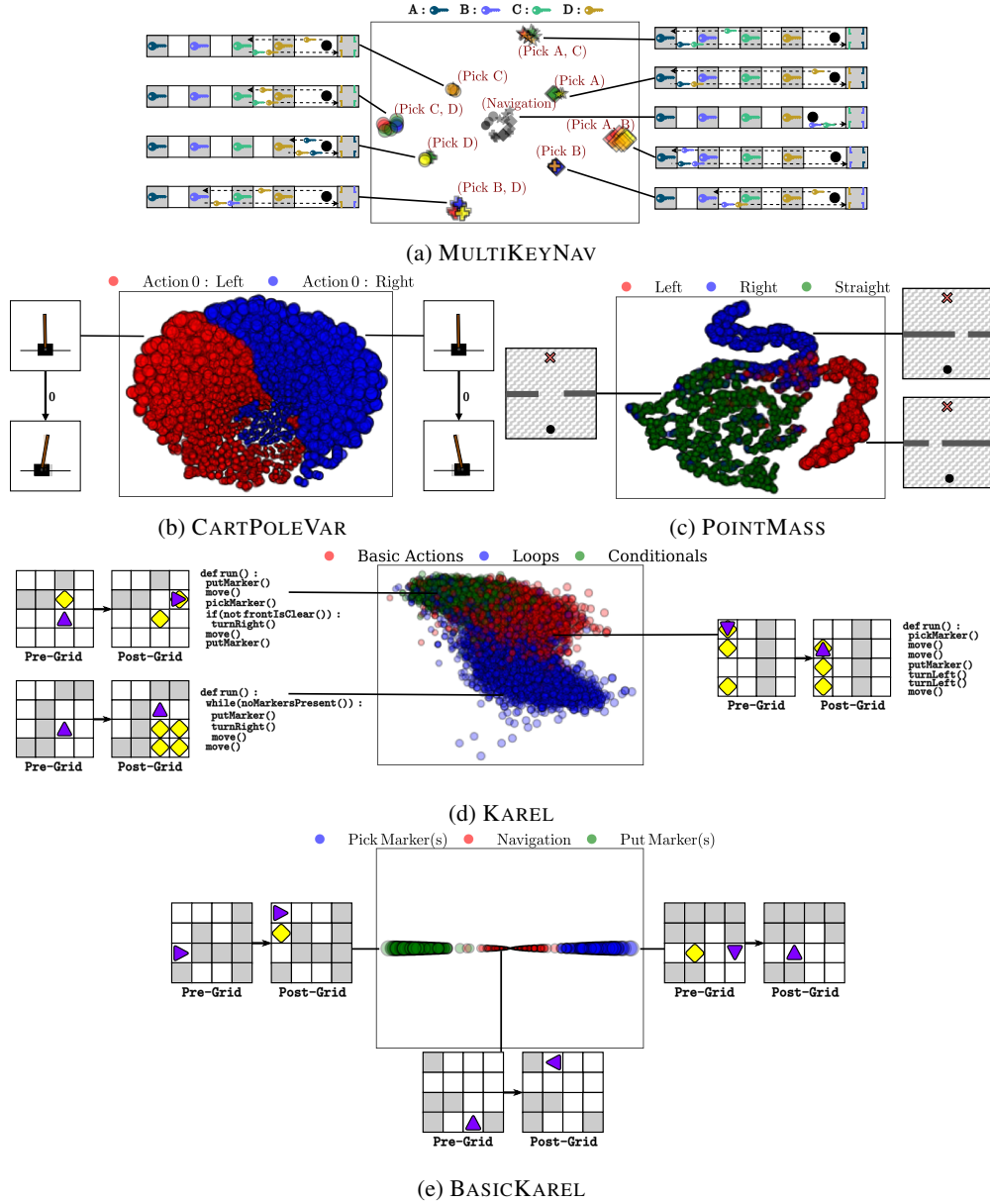


Figure 8: Annotated visualization of the task embedding spaces with example tasks for each cluster.

obtain an agent population of size about 25. The embedding network has two hidden layers (32 neurons in each layer). The embedding dimensionality is 3 with $\mathcal{C}_{\text{NORM}}$.

- KAREL**: For this environment, $\mathcal{S}_{\text{snap}}$ consists of 14681 tasks sampled from the Karel dataset. We combine subpopulations obtained by using all the tasks in $\mathcal{S}_{\text{init}}$, tasks in $\mathcal{S}_{\text{init}}$ that do not require synthesizing token for loops, tasks in $\mathcal{S}_{\text{init}}$ that do not require synthesizing tokens for conditionals, and tasks in $\mathcal{S}_{\text{init}}$ that do not require synthesizing tokens for both loops and conditionals, to obtain an agent population of size about 135. We use the official codebase of [44] to train the agents. The embedding network consists of an input-output encoder (which is the same as that in [44]) followed by a feedforward network with a single hidden layer (256 neurons). The embedding dimensionality is 2 with $\mathcal{C}_{\text{NORM}}$.
- BASICKAREL**: For this environment, $\mathcal{S}_{\text{snap}}$ consists of all the 2400 validation tasks. We combine the subpopulations obtained by masking no action, masking pickMarker, masking putMarker, and masking both pickMarker and putMarker, to obtain an agent population

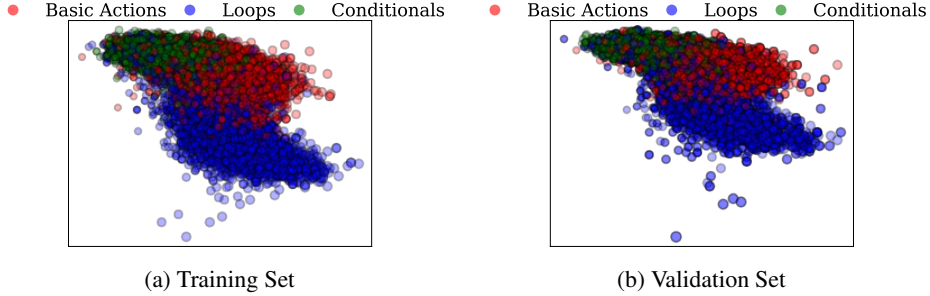


Figure 9: Task embedding spaces obtained using the training and validation sets of tasks for the KAREL environment. This visualization shows that an embedding function learnt using a training set of tasks generalizes to a validation set of tasks.

of size about 55. The embedding network has two hidden layers (32 neurons in each layer). The embedding dimensionality is 1 with $\mathcal{C}_{\text{NORM}}$.

Performance prediction benchmark. We use 10000 samples to estimate the *AA-TA* baseline, 500 samples to estimate the *AD-TA* baseline, 10 samples from each agent in the population to estimate the *AA-TD* baseline, and 10 samples to estimate the *AD-TD* baseline. We evaluate our technique with λ set to 0 (i.e., without $\mathcal{C}_{\text{NORM}}$) on this benchmark since an ordering of the embeddings based on the tasks’ difficulties is not required. β is tuned using the training examples.

Task selection benchmark. We use 100 samples from each agent in the population to estimate mutual information between task optimality variables, and 10 samples from each agent to estimate task difficulty.

E Annotated Visualization of Embedding Spaces

In Figure 8, we present visualizations of the learnt task embedding spaces annotated with an example task for each cluster.

F Generalization Experiment

We present a generalization experiment in which we assess if the embedding function (learnt using a training set of tasks) produces a consistent embedding space for a validation set of tasks. We conduct this evaluation on the KAREL environment by partitioning the tasks into training and validation sets of size 59007 and 14681, respectively. Figure 9 visualizes the task embedding spaces for these sets and shows the generalization ability of the learnt task embedding function.

G Pseudocode for Empirical Estimation of Task Similarity

The pseudocode for the proposed algorithm to empirically estimate \mathcal{I} is given in Algorithm 2. Given an MDP \mathcal{M} and a prior distribution of the agent parameters $p(\theta)$, the algorithm uses N samples to estimate $\mathcal{I}(\mathcal{O}_{s_i, \Theta}; \mathcal{O}_{s_j, \Theta})$. For each sample, the algorithm randomly samples $\theta_l \sim p(\theta)$, and performs rollouts of π_{θ_l} from s_i and s_j to obtain estimates of the probability mass functions required for the computation of \mathcal{I} . Note that $\mathcal{H}_b(p)$ computes the entropy of a Bernoulli random variable X s.t. X takes the value 1 with probability p .

Algorithm 2 Empirically Estimate Task Similarity (\mathcal{I})

1: **procedure** ESTIMATE(Task s_i , Task s_j , MDP \mathcal{M} , Policy π , Prior distribution of the agent parameters $p(\theta)$,
Number of samples N)

2: $n_i \leftarrow 0$ ▷ #successes on s_i

3: $n_j \leftarrow 0$ ▷ #successes on s_j

4: $n_{i_j_1} \leftarrow 0$ ▷ #successes on s_i given success on s_j

5: $n_{i_j_0} \leftarrow 0$ ▷ #successes on s_i given failure on s_j

6: **for** $l \in \{1, \dots, N\}$ **do**

7: Sample agent parameters $\theta_l \sim p(\theta)$ and set it to π .

8: Perform a rollout of π_{θ_l} from s_i on \mathcal{M} .

9: Perform a rollout of π_{θ_l} from s_j on \mathcal{M} .

10: **if** rollout from s_i is a success **then**

11: $n_i \leftarrow n_i + 1$

12: **if** rollout from s_j is a success **then**

13: $n_{i_j_1} \leftarrow n_{i_j_1} + 1$

14: **else**

15: $n_{i_j_0} \leftarrow n_{i_j_0} + 1$

16: **if** rollout from s_j is a success **then**

17: $n_j \leftarrow n_j + 1$

18: $\hat{\mathcal{I}} \leftarrow \mathcal{H}_b\left(\frac{n_i}{N}\right) - \left(\frac{n_j}{N}\right)\mathcal{H}_b\left(\frac{n_{i_j_1}}{n_j}\right) - \left(1 - \frac{n_j}{N}\right)\mathcal{H}_b\left(\frac{n_{i_j_0}}{N - n_j}\right)$

19: **return** $\hat{\mathcal{I}}$
